Hindawi Publishing Corporation
Journal of Nanomaterials
Volume 2014, Article ID 907610, 9 pages
http://dx.doi.org/10.1155/2014/907610

Research Article

Texture-Etched SnO_2 Glasses Applied to Silicon Thin-Film Solar Cells

Bing-Rui Wu,[1] Sin-Liang Ou,[1] Shih-Yung Lo,[1] Hsin-Yuan Mao,[1] Jhen-Yu Yang,[1] and Dong-Sing Wuu[1,2]

[1] *Department of Materials Science and Engineering, National Chung Hsing University, 250 Kuo Kuang Road, Taichung 40227, Taiwan*
[2] *Department of Materials Science and Engineering, Da-Yeh University, Changhua 51591, Taiwan*

Correspondence should be addressed to Dong-Sing Wuu; dsw@dragon.nchu.edu.tw

Received 13 December 2013; Revised 8 February 2014; Accepted 9 February 2014; Published 18 March 2014

Academic Editor: Sheng-Po Chang

Transparent electrodes of tin dioxide (SnO_2) on glasses were further wet-etched in the diluted HCl:Cr solution to obtain larger surface roughness and better light-scattering characteristic for thin-film solar cell applications. The process parameters in terms of HCl/Cr mixture ratio, etching temperature, and etching time have been investigated. After etching process, the surface roughness, transmission haze, and sheet resistance of SnO_2 glasses were measured. It was found that the etching rate was increased with the additions in etchant concentration of Cr and etching temperature. The optimum texture-etching parameters were 0.15 wt.% Cr in 49% HCl, temperature of 90°C, and time of 30 sec. Moreover, silicon thin-film solar cells with the p-i-n structure were fabricated on the textured SnO_2 glasses using hot-wire chemical vapor deposition. By optimizing the texture-etching process, the cell efficiency was increased from 4.04% to 4.39%, resulting from the increment of short-circuit current density from 14.14 to 15.58 mA/cm^2. This improvement in cell performances can be ascribed to the light-scattering effect induced by surface texturization of SnO_2.

1. Introduction

Owing to the advantages consisting of low cost, easy fabrication, and environmental friendliness, silicon (Si) is a very promising material for the photovoltaic applications [1, 2]. Thin-film solar cells based on amorphous silicon (a-Si) or microcrystalline silicon (μc-Si) are the most popular products applied to the building-integrated photovoltaics and consumer electronics. Transparent conductive oxide (TCO) films are usually used as the front electrode of thin-film solar cells. For a transparent electrode, the requirements of TCO films are a low sheet resistance (R_{sheet}) to minimize the current loss, a low contact resistance to semiconductor layers, and a high transmission of incident light. To completely utilize the incident light, an important technique of the so-called light trapping has been developed using a TCO with suitable surface texture. Schematic diagrams of the light-scattering effects in roughened and smooth TCO glasses are shown in Figure 1. It was indicated that a specific design of TCO films plays an important role in enhancing the performances of thin-film solar cells. A surface-textured TCO can scatter the light greatly and increase the effective optical path length within the active layers [3–6]. A rough TCO film also ensures that the roughness is copied by the film deposited on it, so that the back metal electrode produces an increased scattering of reflected light. Therefore, this would improve both the optical absorption and current density in thin-film solar cells. After that, various randomly textured TCO substrates have been proposed to increase the light scattering. As-deposited and postchemical textured TCOs are both useful to achieve the rough substrates. The common TCO materials applied to thin-film solar cells consist of tin dioxide (SnO_2) [6] and zinc oxide (ZnO) [7, 8]. The great majority of glass-based Si thin-film modules are prepared on the fluorine-doped SnO_2 (SnO_2:F) glasses due to their intrinsic rough surface [4, 5]. Moreover, the directly deposited or texture-etched ZnO is another attractive method for the fabrication of rough TCO substrate [9–12]. By using the texture-etched ZnO, the quantum efficiency of thin-film solar cells over the whole spectral range can be increased [11, 12]. A further

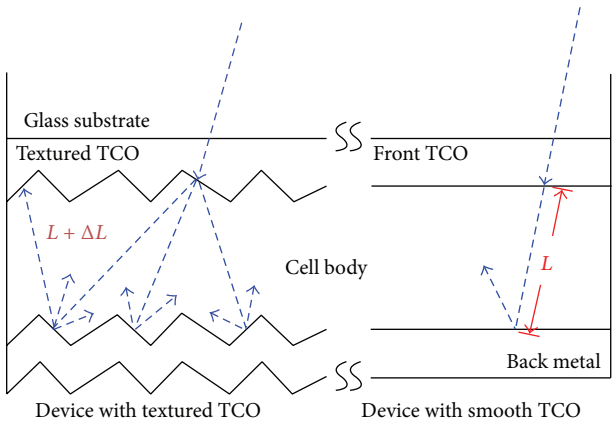

Figure 1: Schematic diagrams of the light-scattering effects in roughened and smooth TCO glasses.

improvement in the reduction of free carrier absorption losses in the red/IR and absorption around the optical edge of ZnO in the blue/UV region can be achieved [13].

SnO_2, one of the most common TCO films, is usually prepared by atmospheric pressure chemical vapor deposition (APCVD) with a natively textured surface [14]. Asahi type-U glass is a worldwide TCO substrate for thin-film solar cell industry, which is a natively textured SnO_2 glass with the great light scattering of 10% in transmission haze ratio. A method to create a pattern or to remove the SnO_2 layer by wet etching has been reported [15]. The etchant of this method includes 3 liters of 50% HCl and 20 g of chromium metal (Cr). The mixture is heated to 90°C with constant stirring to dissolve the Cr. The overall reaction sequence of the etching treatment is given by the following equation:

$$2Cr^{++} + Sn^{++++} \longrightarrow 2Cr^{+++} + Sn^{++}, \quad (1)$$

where the SnO_2 is stannic oxide (Sn^{++++}) and is transferred to stannous oxide (Sn^{++}) after the etching reaction. The stannous oxide can be soluble in the acid solution to complete the etching reaction.

In this study, we choose the mass-produced SnO_2 soda glasses as substrates which were usually used for the building-integrated photovoltaic applications. Then the wet chemical texturization was performed by using the diluted HCl:Cr solution to reach larger surface roughness and better light-scattering properties for thin-film solar cell applications. The etching parameters, such as etchant concentration, etching temperature, and etching time (t_{etch}), were investigated. Moreover, Si thin-film solar cells with p-i-n structure on various textured SnO_2 glasses were fabricated and their characteristics were also studied.

2. Experimental Procedure

The 3-mm thick soda glasses with APCVD-deposited 600 nm thick SnO_2 films were chosen as the substrates. These SnO_2 glasses showed the high conductivity of 12–14 Ω/□ and high transparency of >85% in the 400–800 nm wavelength range. The roughness and transmission haze of SnO_2 films were about 260 nm and 7%, respectively. To obtain the textured surface, the SnO_2 glasses were etched in a SnO_2 etchant. Various Cr concentrations from 0.05 to 1 wt.% were mixed into the diluted HCl (49%) to prepare the SnO_2 etchants. The etching temperature was varied from room temperature to 100°C. Moreover, the t_{etch} was increased from 1 to 300 sec. By changing these parameters, the effects of etching conditions on the optoelectronic performances of SnO_2 films were investigated in detail. The ability of the textured SnO_2 films to scatter light can be expressed by the transmission haze ratio (H_t):

$$\text{Transmission haze } (H_t) = \frac{\text{Diffuse transmittance}}{\text{Total transmittance}}, \quad (2)$$

where the transmission haze is defined as the percentage of transmitted light deviated from the incident beam by more than 2.5° from the normal incident beam. In this study, the total transmittance was measured by using an integrating sphere. The diffuse transmittance was calculated by the difference between the total and direct transmittance. Considering the rough surface of SnO_2, the etching depth was measured repeatedly by an α-step surface profiler to determine the average etching rate. Field-emission scanning electron microscope (FE-SEM, JEOL JSM-6700F) was used to observe the SnO_2 morphology. An atomic force microscopy (AFM, Agilent 5400) was applied for the measurement of surface roughness. The R_{sheet} of textured SnO_2 film was investigated by using the four-point probe method.

Subsequently, Si thin-film solar cells were fabricated on the textured SnO_2 films. The fabrication process can be divided into three main steps: SnO_2 texture etching, deposition of the Si p-i-n structure, and formation of the back electrode. The p-type, intrinsic and n-type Si layers in this study were prepared in a single chamber hot-wire chemical vapor deposition (HWCVD) system. The HWCVD technique is widely employed as the fabrication of Si-based thin films consisting of a-Si [16], μc-Si [17], doped Si [18], and silicon carbide (SiC) [19]. Due to the unique advantages including crystalline film deposition at low substrate temperature, high deposition rate, and high gas utilization in HWCVD [20], it has attracted great attention for its potential applications in thin-film solar cells [21, 22] and transistors [23, 24]. In our previous studies, HWCVD was used to deposit the Si-based films for various purposes, such as aluminum induced crystallization [25], n-type μc-Si [26], p-type window layers (nanocrystalline Si [27] and SiC [28]), and heterojunction solar cells [29]. Before loading the SnO_2 substrate into HWCVD system, the chamber was firstly treated using the atomic H generated from H_2 gas [30]. Table 1 summarizes the process parameters of HWCVD-deposited p-, i-, and n-type Si and buffer layers. The key parameters of Si film deposition include a wire temperature of 1700°C, a substrate temperature of 300°C, and the working pressure of 100 mTorr. Silane (SiH_4) was applied to the source gas with flow rate (Φ_{SiH_4}) of 2 sccm. Phosphine (PH_3, 1% in H_2) and diborane (B_2H_6, 1% in H_2) were used as the dopant gases with flow rates (Φ_{dopant}) of 18 and 20 sccm, respectively, to prepare n-type and p-type microcrystalline Si layers, which were reported

Table 1: Deposition parameters and properties of p-, i-, n-type Si and buffer layers by HWCVD.

Film	Unit	p-layer	Buffer	i-layer	n-layer
Filament temperature	˚C	1700	1700	1700	1700
Substrate temperature	˚C	300	300	300	300
Pressure	mTorr	100	100	100	100
Gas flow rate (Φ)	sccm	$\Phi_{SiH_4} = 2$ $\Phi_{B_2H_6} = 20$	$\Phi_{SiH_4} = 1$ $\Phi_{CH_4} = 1$ $\Phi_{B_2H_6} = 3$ $\Phi_{H_2} = 20$	$\Phi_{SiH_4} = 2$	$\Phi_{SiH_4} = 2$ $\Phi_{PH_3} = 18$
Energy gap	eV	1.97	2.18	1.68	1.78
Crystalline fraction	%	67	59	Amorphous	57
Deposition rate	nm/sec	0.201	0.208	0.262	0.213
Hall concentration	cm^{-3}	1×10^{20}	5×10^{19}	—	4×10^{19}

elsewhere [25, 27–29]. Some characteristics consisting of energy gap (by Tauc plot), crystalline fraction (by Raman spectroscopy), deposition rate (by profilometer), and Hall concentration (by Hall measurement) of these films were also exhibited in Table 1. The detailed experimental procedures and similar discussions in these films characteristics were presented in our previous works [25, 27–29]. Between the p- and i-layers, a 10 nm thick p-type microcrystalline SiC buffer layer with energy gap of 2.18 eV was deposited for better band structure. The main benefit of this buffer layer originated from its effect on the electric field distribution, which minimized the recombination near the p/i interface [31]. Compared to the literatures [32, 33], the energy gap of our buffer was in good agreement with that of crystalline cubic silicon carbide (3C-SiC). Details of the HWCVD-deposited SiC were reported in our previous work [28]. The thicknesses of p-, i-, and n-layers were 30, 500, and 50 nm, respectively. Such an insufficient i-layer thickness of 500 nm was used to induce an incomplete absorption. It can provide an investigation of the light-scattering and absorption effects in a limited thickness of absorber layer. After depositing the p-i-n structure, the 500 nm thick Ag and 1-μm thick Al layers were grown sequentially as the back electrode by electron-beam evaporation and then annealed at 500˚C to achieve an ohmic contact. Finally, Si thin-film solar cells were fabricated with the structure of glass/textured SnO_2/p-i-n Si layers/Ag-Al and the cell size was $5 \times 5\,mm^2$. Device performances consisting of current density voltage (J-V) and external quantum efficiency (EQE) of solar cells were measured by Keithley 2400 SourceMeter (Sciencetech, model SS150W) with a one-sun AM1.5G light source (100 mW/cm^2) at room temperature.

3. Results and Discussion

This study investigated the improvement in optical characterization of SnO_2 films with the optimized textured surface to enhance the spectral response and efficiency of thin-film solar cells. In order to control the etching rate, various SnO_2 etchants and etching temperatures were used. As mentioned above, the etchants with various Cr concentrations from 0.05 to 1 wt.% were employed to etch the SnO_2 films. When the Cr concentration was less than 0.15 wt.%, a poor etching rate approaching to no etching was found on the film surface. On the other hand, the etching reaction was violent for the Cr concentration more than 0.45 wt.%, leading to a low reproduction in the textured surface. The stable and high reproducible etching reactions have taken place by using the etchants with Cr concentration of 0.15–0.45 wt.%. Therefore, the etchants with Cr concentrations of 0.15, 0.3, and 0.45 wt.% denoted as etchants A, B, and C, respectively, were chosen to further etch the SnO_2 films with various etching conditions (temperature and time). Figure 2 shows the average etching rates of these etchants at various etching temperatures. It was found that the etching reaction appeared when the process temperature was higher than 60˚C. Etching rates of these three etchants were all increased with increasing the temperature. As the temperature was increased from 60 to 100˚C, the etching rates of etchants A, B, and C rose from 31.4, 74.5, and 89.2 to 121, 158, and 188.6 nm/min, respectively. The higher Cr concentration and temperature would result in a higher etching rate.

Various temperatures and t_{etch} were carried out for etchants A, B, and C to optimize the roughness and H_t properties of SnO_2 films. After comparing all etching results, the higher root-mean-square (RMS) roughnesses and H_t values were observed at 90, 80, and 80˚C for etchants A, B, and C, respectively. The RMS roughnesses of SnO_2 films etched in these three etchants with their optimum temperatures at various t_{etch} were shown in Figure 3. Several t_{etch} of 1, 5, 15, 30, 60, 120, and 300 sec were used in the etching treatments. From the results, the RMS roughness of SnO_2 with these three etchants showed the similar trend to each other. In the range of 1–120 sec, the RMS roughness of SnO_2 was firstly increased and then decreased. Because the etching reaction was started at the grain boundaries of film, it induced an increment in RMS in the beginning. The following decrease in RMS with increasing the t_{etch} to 120 sec was probably ascribed to the isotropic etching in some sharp regions of the grains, causing a smoother surface. After etching for 300 sec, we found that the RMS was increased again. It could result from the severe damage on SnO_2 surface during long-time etching. For the changes in surface morphology mentioned above, it will be displayed later in SEM images. The highest roughness value

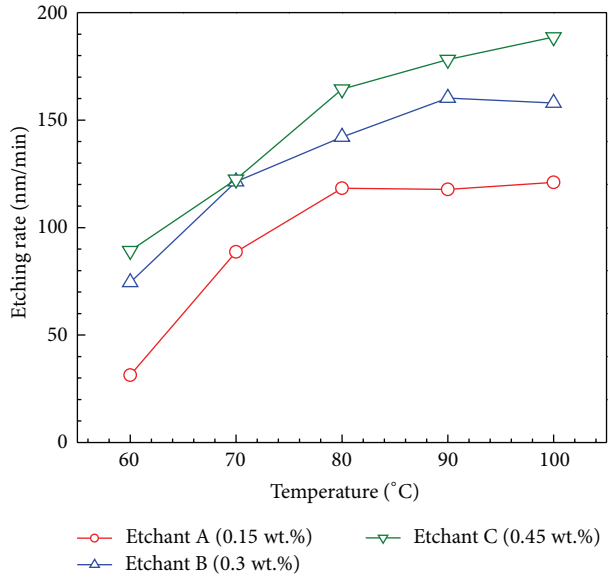

FIGURE 2: Etching rates for SnO_2 films in etchants A, B, and C as a function of the etching temperature.

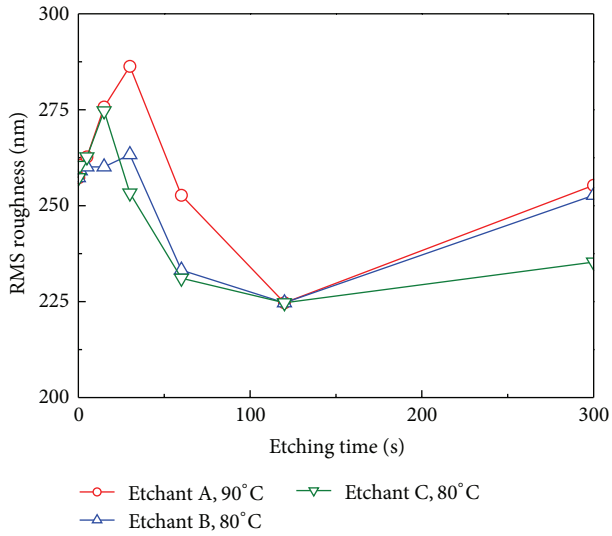

FIGURE 3: Surface RMS roughnesses of etched SnO_2 glasses in etchants A, B, and C with their optimum temperatures as a function of etching time.

of 286.3 nm was obtained using the etchant A for 30 sec. For etchants B and C, the highest roughness values of 263.3 and 274.7 nm were found after etching for 30 and 15 sec, respectively.

The average H_t values (@ 550 nm) of SnO_2 glasses etched by various etchants as a function of t_{etch} were shown in Figure 4. It was found that the H_t curves exhibited the similar trends to the results of RMS roughness displayed in Figure 3. In the case of sample treated with etchant A, the H_t increased with an increment of t_{etch} from 1 to 30 sec. Further, increasing the t_{etch} from 30 to 300 sec, the H_t firstly decreased and then increased. Two relatively high H_t values of 8.38% and 9.13%

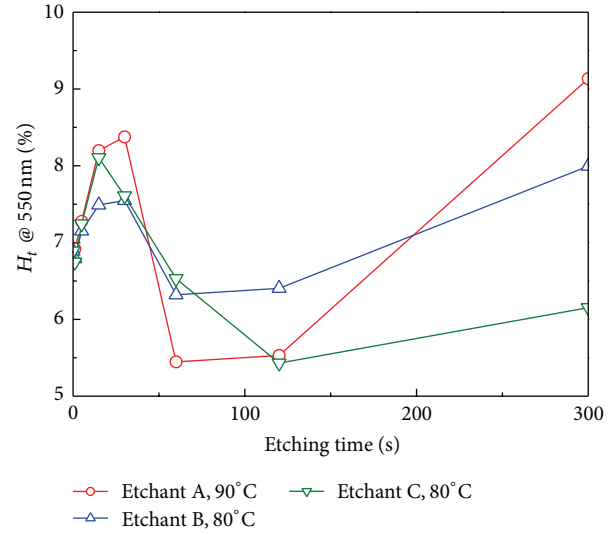

FIGURE 4: Transmission haze (@ 550 nm) of etched SnO_2 glasses in etchants A, B, and C as a function of etching time.

were observed at the t_{etch} of 30 and 300 sec, respectively. Moreover, for the uses of etchants B and C to our samples, the results demonstrated the similar tendency to each other. The highest H_t of samples treated with etchants B and C were 7.55 and 8.1% after etching for 30 and 15 sec, respectively.

The etched SnO_2 surface was visualized by the FE-SEM and AFM. Figures 5(a), 5(b), 5(c), and 5(d) showed the SEM images of SnO_2 etched in the etchant A at 90°C for 0, 30, 120, and 300 sec, respectively. The AFM images of same samples were shown in Figures 6(a)–6(d). The RMS and R_{sheet} of original SnO_2 are measured to be 260 nm and 13.2 Ω/□, respectively. As displayed in Figures 5(c) and 6(c), some small holes appeared in the SnO_2 grains as the t_{etch} was increased to 120 sec. For the 300 sec etching sample, the size of holes was grown up to several hundreds of nanometers as shown in Figures 5(d) and 6(d). In comparison to the nonetching sample, the grain shapes of SnO_2 with etching for 30 sec were clearer because the etching usually started at the grain boundaries. After etching for 120 sec, the grains became smoother owing to the isotropic nature of wet etching. Nevertheless, with increasing the t_{etch} to 300 sec, the formation of voids can be observed. This indicated that the SnO_2 suffered long-time damage by wet chemical etching. These voids may lead to more large-angle scattering light. This could be the reason why these samples with the t_{etch} of 300 sec exhibited a larger increment in H_t than that in RMS roughness. These surface morphologies of SnO_2 films with the t_{etch} from 0 to 300 sec can reflect the various degrees of surface roughness, which is in good agreement with the results shown in Figure 3. The R_{sheet} values of SnO_2 etched for 30, 120, and 300 sec were 13.9, 15.1, and 27.6 Ω/□, respectively. Apparently, the R_{sheet} increased with increasing the t_{etch} and hence induced a detrimental effect on the application of thin-film solar cells. As the etching process was performed for 300 sec, there existed a rapid increase in R_{sheet} due to the chemical damages caused by the long-time etching, as shown

Table 2: Light J-V parameters of silicon p-i-n thin-film solar cells deposited on texture-etched SnO_2 with various t_{etch}.

t_{etch} (s)	H_{t550} (%)	R_{sheet} (Ω/□)	η (%)	V_{oc} (V)	J_{sc} (mA/cm^2)	FF (%)	R_s (Ω)
Original	6.9	13.2	4.04	0.52	14.14	54.94	11.06
30	8.38	13.9	4.39	0.52	15.58	54.24	10.88
120	5.53	15.1	4.04	0.50	16.22	49.78	11.76
300	9.13	27.6	3.48	0.49	14.99	47.41	17.66

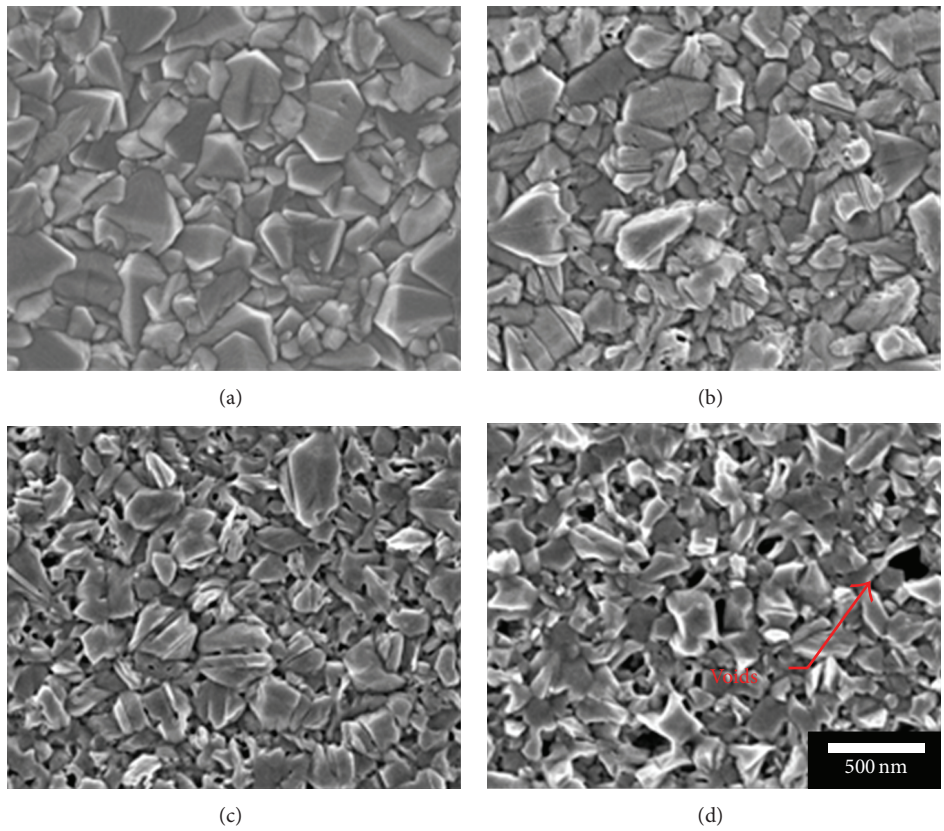

Figure 5: FE-SEM images of SnO_2 etched in the etchant A at 90°C for (a) 0, (b) 30, (c) 120, and (d) 300 sec.

in Figures 5(d) and 6(d). Based on the H_t, R_{sheet}, and surface roughness of etched SnO_2, the t_{etch} of 30 sec could be an optimum condition in this study.

In order to investigate the improvement in light scattering, the 500 nm thick a-Si films were deposited upon SnO_2 glasses with and without texture etching. For the measurements of total transmittance (T) and total reflectance (R) by the integrating sphere, the samples were illuminated from the glass side. A calculated value of 1-R-T represented the absorbance of this SnO_2 glass with a 500 nm thick a-Si layer. The value indicated the real quantity of light trapping or light harvesting ability for 500 nm thick a-Si on a rough SnO_2 substrate. It also revealed that the effect of light scattering was modified by wet texturization. The 1-R-T and H_t values of original and etched SnO_2 glasses were shown in Figure 7. We found that both 1-R-T and H_t of etched SnO_2 for 30 sec were higher than those of the other samples in the visible range of 400–800 nm. It proved that there was an increment in diffuse transmittance for surface-roughened SnO_2 glass. In addition, the absorbance of 500 nm thick a-Si for incident light was improved via the scattering effect. The effects of texturization on optical characteristics were similar to the results of previous research [34]. From our observation, the sample which used etched SnO_2 with etchant A at 90°C for 30 sec has higher 1-R-T value than that of the others. Thus, we chose the etchant A with the optimum conditions (etching temperature of 90°C and t_{etch} of 30 sec) as the standard texture-etching process.

To demonstrate the suitability of textured SnO_2 glasses for thin-film solar cell applications, p-i-n solar cells have been fabricated by HWCVD on original and etched SnO_2 glasses with a 500 nm thick intrinsic absorber layer. Table 2 summarizes the performances of the p-i-n solar cells deposited on SnO_2 glasses etched with various t_{etch}. From the measurements shown in Table 2, there existed an increment in R_{sheet} of TCO from 13.2 to 27.6 Ω/□ as the t_{etch} was increased from 0 to 300 sec. It can be expected that the series resistance of cell would increase with increasing the R_{sheet} of TCO, further

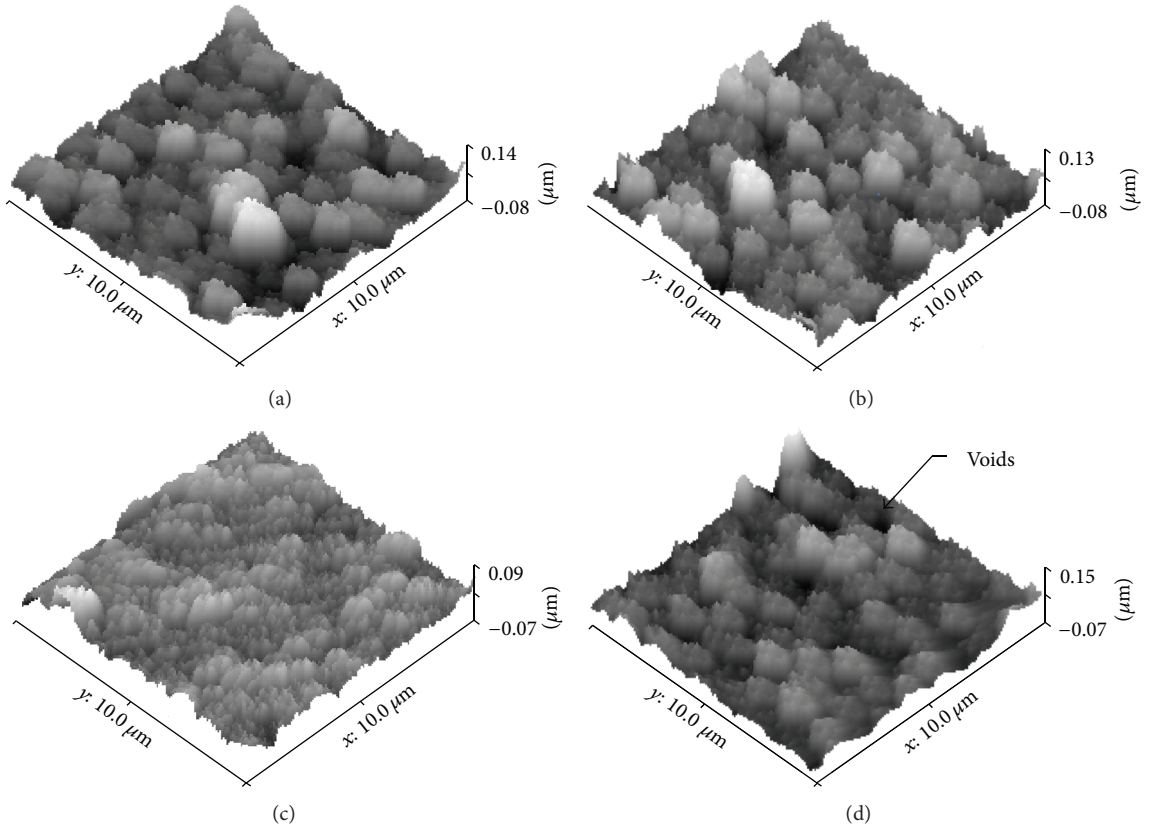

FIGURE 6: AFM images of SnO_2 etched in the etchant A at 90°C for (a) 0, (b) 30, (c) 120, and (d) 300 sec.

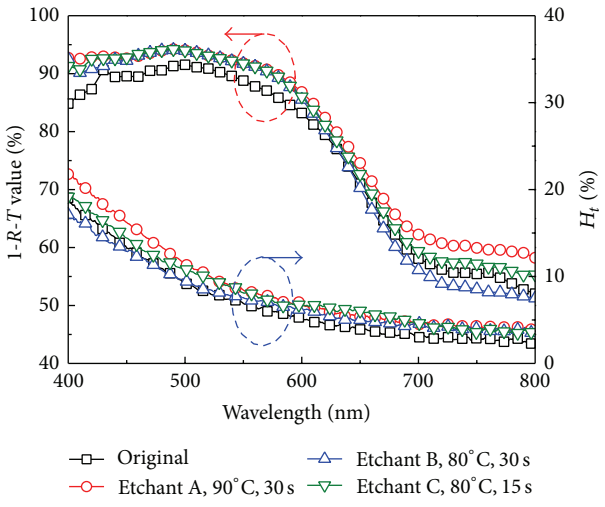

FIGURE 7: Transmission haze and 1-R-T values of original and etched SnO_2 glasses in the visible range of 400–800 nm.

leading to the decreases in fill factor (FF) and conversion efficiency (η). In fact, the cell performances in our work are mainly influenced by both R_{sheet} and roughness of TCO. Generally, the short-circuit current density (J_{sc}) of cell can be enhanced by using textured TCO substrate because of the light scattering generated from the rough surface. However, it also results in the deteriorations in open-circuit voltage (V_{oc}) and FF of cell [35]. Therefore, it is important to control an acceptable degree of substrate texturization, which can both improve the J_{sc} and induce the minimum deteriorations in V_{oc} and FF of cell. As shown in Table 2, the V_{oc} and FF values of cell with substrate etching for 30 sec were similar to those with nonetched substrate. Nevertheless, with the assistance of etching process for 30 sec to the SnO_2 substrate, the J_{sc} was increased from 14.14 to 15.58 mA/cm^2, while the cell efficiency was increased from 4.04% to 4.39%. It confirmed that the t_{etch} of 30 sec was indeed the optimum parameter for substrate texturization in our study. On the other hand, although the J_{sc} of the samples with substrate etching for 30 and 120 sec were close to each other, there was a considerable difference in their FF values. It can be seen that the cell using long-time (120 sec) etched substrate had the worse FF value of 49.78% than that with substrate etching for 30 sec (54.24%). The deteriorated FF value in the sample with substrate etching for 120 sec could be attributed to the higher R_{sheet} and lower surface roughness of TCO. This revealed that the better light trapping which resulted from the rougher SnO_2 surface (wet etching for 30 sec) can lead to the highest current density of cell device. Moreover, the series resistances (R_s) of 11.06, 10.88, 11.76, and 17.66 Ω were also given in Table 2 for the samples with non-, 30 sec, 120 sec, and 300 sec etched SnO_2 substrates, respectively. It was obvious that the much higher

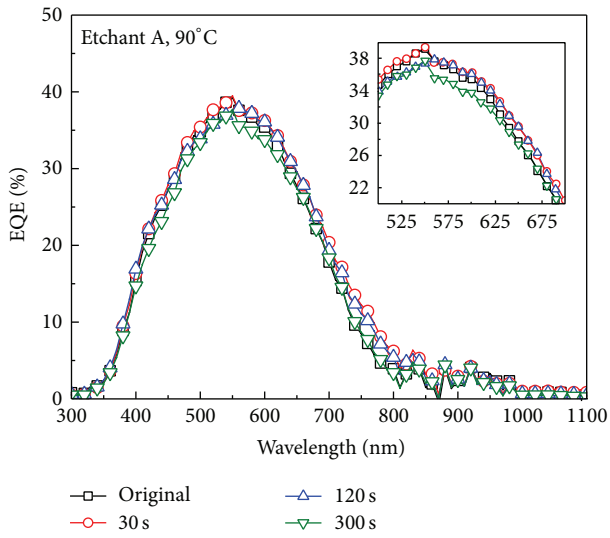

FIGURE 8: EQE characteristics of Si p-i-n solar cells deposited on SnO_2 glasses with original and textured (etched in etchant A at 90°C for 30–300 sec) surfaces as a function of measured wavelength. The inset is an enlarged view of Figure 8 focused on the measured wavelength region of 500–700 nm.

R_s in the sample with the t_{etch} of 300 sec was attributed to the long-time etching, resulting in more severe damage on SnO_2 surface.

Figure 8 shows the EQE characteristics of solar cells deposited on the original and textured SnO_2 glasses. As compared with the solar cell on original SnO_2 glass, the device prepared on the 30 sec etched SnO_2 exhibited an increase in EQE for almost full range from 300 to 1100 nm. As can be known, the elevation in EQE can enhance the J_{sc} performance directly. An enlarged view of Figure 8 focused on the measured wavelength region of 500–700 nm was displayed in the inset. We can find that the cell with 30 sec etched substrate presented a higher EQE value in almost full wavelength ranging from 300 to 900 nm. However, based on the previous study, a-Si solar cell has a low absorption around the wavelength of 800 nm [36]. Therefore, it can be assumed that the main contribution in EQE for texturized cell happened from near-ultraviolet region to red region (300–750 nm), which was in good agreement with previous research [37]. This appearance was similar to the 1-R-T value shown in Figure 7. This proved again that the enhancement in J_{sc} mainly resulted from the light-scattering effect inside of absorber layer by using the textured SnO_2 substrate. Furthermore, the η of cell devices can be improved from 4.04% to 4.39% as the t_{etch} was increased from 0 to 30 sec.

4. Conclusion

A wet chemical etching technique using a diluted HCl:Cr mixture was applied to the surface texturization of SnO_2 glass to enhance the light scattering. It was found that the etchant concentration, etching temperature, and etching time can influence the optoelectronic properties of SnO_2 films. From our measurement, the etching rate was increased with increasing the etchant concentration of Cr and etching temperature. The etchant with appropriate Cr concentration and etching parameters would lead to the good textured surface and optical characterization. The optimum etching parameters in this work were 0.15 wt.% Cr in 49% HCl, temperature of 90°C, and time of 30 sec. With increasing the etching time, the resistance of SnO_2 was increased because of the excessive damage to film surface. Moreover, as the optimum etching parameters were used for the surface texturization, the SnO_2 glass showed a better transmission haze of 8.38% as compared to that of original SnO_2 (7%). Meanwhile, by employing the optimum textured surface, the J_{sc} of 15.58 mA/cm^2, the V_{oc} of 0.52 V, the FF of 54.24%, and the η of 4.39% can be obtained in the thin-film solar cell with a 500 nm thick absorber. It presented about 8.7% increment in cell efficiency as compared with that using the original SnO_2 glass (η = 4.04%). According to the EQE result, this improvement was mainly due to the light absorption in red and infrared regions. It was confirmed that the roughness of APCVD-deposited-SnO_2 surface can be moderately increased using wet chemical etching in a HCl : Cr solution. Additionally, with the employment of optimum textured parameters to SnO_2 surface, there is a positive influence on the light scattering. This can lead to the enhancements in current density and conversion efficiency of thin-film solar cell.

Conflict of Interests

The authors declare that there is no conflict of interests regarding the publication of this paper.

Acknowledgment

This research was supported by the National Science Council of Taiwan, under Contract no. NSC 99-2221-E-005-101-MY3.

References

[1] C. M. Lee, S. P. Chang, S. J. Chang, and C. I. Wu, "High-efficiency si solar cell fabricated by ion implantation and inline backside rounding process," *International Journal of Photoenergy*, vol. 2012, Article ID 670981, 7 pages, 2012.

[2] C. M. Lee, S. P. Chang, S. J. Chang, and C. I. Wu, "p-type quasi-mono silicon solar cell fabricated by ion implantation," *International Journal of Photoenergy*, vol. 2013, Article ID 171390, 8 pages, 2013.

[3] B. Rech, T. Repmann, M. N. van den Donker et al., "Challenges in microcrystalline silicon based solar cell technology," *Thin Solid Films*, vol. 511-512, pp. 548–555, 2006.

[4] J. Müller, B. Rech, J. Springer, and M. Vanecek, "TCO and light trapping in silicon thin film solar cells," *Solar Energy*, vol. 77, no. 6, pp. 917–930, 2004.

[5] K. Yamamoto, A. Nakajima, M. Yoshimi et al., "A high efficiency thin film silicon solar cell and module," *Solar Energy*, vol. 77, no. 6, pp. 939–949, 2004.

[6] T. Matsui, M. Tsukiji, H. Saika, T. Toyama, and H. Okamoto, "Influence of substrate texture on microstructure and photovoltaic performances of thin film polycrystalline silicon solar cells," *Journal of Non-Crystalline Solids*, vol. 299–302, no. 2, pp. 1152–1156, 2002.

[7] T. Söderström, F.-J. Haug, V. Terrazzoni-Daudrix, and C. Ballif, "Optimization of amorphous silicon thin film solar cells for flexible photovoltaics," *Journal of Applied Physics*, vol. 103, no. 11, Article ID 114509, 2008.

[8] M. Berginski, J. Hüpkes, M. Schulte et al., "The effect of front ZnO:Al surface texture and optical transparency on efficient light trapping in silicon thin-film solar cells," *Journal of Applied Physics*, vol. 101, no. 7, Article ID 074903, 2007.

[9] J. Müller, G. Schöpe, O. Kluth et al., "Upscaling of texture-etched zinc oxide substrates for silicon thin film solar cells," *Thin Solid Films*, vol. 392, no. 2, pp. 327–333, 2001.

[10] Y. C. Lin, Y. C. Jian, and J. H. Jiang, "A study on the wet etching behavior of AZO (ZnO:Al) transparent conducting film," *Applied Surface Science*, vol. 254, no. 9, pp. 2671–2677, 2008.

[11] O. Kluth, B. Rech, L. Houben et al., "Texture etched ZnO:Al coated glass substrates for silicon based thin film solar cells," *Thin Solid Films*, vol. 351, no. 1-2, pp. 247–253, 1999.

[12] Y. Wang, X. Zhang, L. Bai, Q. Huang, C. Wei, and Y. Zhao, "Effective light trapping in thin film silicon solar cells from textured Al doped ZnO substrates with broad surface feature distributions," *Applied Physics Letters*, vol. 100, no. 26, Article ID 263508, 2012.

[13] J. Springer, B. Rech, W. Reetz, J. Müller, and M. Vanecek, "Light trapping and optical losses in microcrystalline silicon pin solar cells deposited on surface-textured glass/ZnO substrates," *Solar Energy Materials and Solar Cells*, vol. 85, no. 1, pp. 1–11, 2005.

[14] R. G. Gordon, J. Proscia, F. B. Ellis Jr., and A. E. Delahoy, "Textured tin oxide films produced by atmospheric pressure chemical vapor deposition from tetramethyltin and their usefulness in producing light trapping in thin film amorphous silicon solar cells," *Solar Energy Materials*, vol. 18, no. 5, pp. 263–281, 1989.

[15] P. W. Simon, "Etchant and method of etching tin oxide film," Burroughs Corporation, U.S. Patent 4,009,061, 1977.

[16] A. H. Mahan, J. Carapella, B. P. Nelson, R. S. Crandall, and I. Balberg, "Deposition of device quality, low H content amorphous silicon," *Journal of Applied Physics*, vol. 69, no. 9, pp. 6728–6730, 1991.

[17] R. O. Dusane, S. R. Dusane, V. G. Bhide, and S. T. Kshirsagar, "Hydrogenated microcrystalline silicon films produced at low temperature by the hot wire deposition method," *Applied Physics Letters*, vol. 63, no. 16, pp. 2201–2203, 1993.

[18] J. P. Conde, P. Alpuim, M. Boucinha, J. Gaspar, and V. Chu, "Amorphous and microcrystalline silicon deposited by hot-wire chemical vapor deposition at low substrate temperatures: application to devices and thin-film microelectromechanical systems," *Thin Solid Films*, vol. 395, no. 1-2, pp. 105–111, 2001.

[19] T. Wu, H. Shen, B. Cheng, Y. Pan, C. Gao, and J. Shen, "Effect of filament temperature on properties of hot wire CVD deposited nc-3C-SiC films from SiH4-C2H2-H2 mixture," *Materials Research Innovations*, vol. 16, no. 3, pp. 165–169, 2012.

[20] S. K. Soni, A. Phatak, and R. O. Dusane, "High deposition rate device quality a-Si:H films at low substrate temperature by HWCVD technique," *Solar Energy Materials and Solar Cells*, vol. 94, no. 9, pp. 1512–1515, 2010.

[21] B. Schroeder, "Status report: solar cell related research and development using amorphous and microcrystalline silicon deposited by HW(Cat)CVD," *Thin Solid Films*, vol. 430, no. 1-2, pp. 1–6, 2003.

[22] T. Chen, Y. Huang, D. Yang, R. Carius, and F. Finger, "Microcrystalline silicon thin film solar cells with microcrystalline silicon carbide window layers and silicon absorber layers both prepared by Hot-Wire CVD," *Physica Status Solidi: Rapid Research Letters*, vol. 4, no. 3-4, pp. 61–63, 2010.

[23] M. Fonrodona, D. Soler, J. Escarré et al., "Low temperature amorphous and nanocrystalline silicon thin film transistors deposited by Hot-Wire CVD on glass substrate," *Thin Solid Films*, vol. 501, no. 1-2, pp. 303–306, 2006.

[24] B. Stannowski, J. K. Rath, and R. E. I. Schropp, "Thin-film transistors deposited by hot-wire chemical vapor deposition," *Thin Solid Films*, vol. 430, no. 1-2, pp. 220–225, 2003.

[25] B. R. Wu, S. Y. Lo, D. S. Wuu et al., "Direct growth of large grain polycrystalline silicon films on aluminum-induced crystallization seed layer using hot-wire chemical vapor deposition," *Thin Solid Films*, vol. 520, no. 18, pp. 5860–5866, 2012.

[26] S.-Y. Lien, D.-S. Wuu, B.-R. Wu, R.-H. Horng, M.-C. Tseng, and H.-H. Yu, "Hot-wire CVD deposited n-type μc-Si films for μc-Si/c-Si heterojunction solar cell applications," *Thin Solid Films*, vol. 516, no. 5, pp. 765–769, 2008.

[27] H.-Y. Mao, S.-Y. Lo, D.-S. Wuu et al., "Hot-wire chemical vapor deposition and characterization of p-type nanocrystalline Si films for thin film photovoltaic applications," *Thin Solid Films*, vol. 520, no. 16, pp. 5200–5205, 2012.

[28] H.-Y. Mao, D.-S. Wuu, B.-R. Wu, S.-Y. Lo, H.-Y. Hsieh, and R.-H. Horng, "Hot-wire chemical vapor deposition and characterization of p-type nanocrystalline SiC films and their use in Si heterojunction solar cells," *Thin Solid Films*, vol. 520, no. 6, pp. 2110–2114, 2012.

[29] S.-Y. Lien, B.-R. Wu, J.-C. Liu, and D.-S. Wuu, "Fabrication and characteristics of n-Si/c-Si/p-Si heterojunction solar cells using hot-wire CVD," *Thin Solid Films*, vol. 516, no. 5, pp. 747–750, 2008.

[30] A. Masuda and H. Matsumura, "Guiding principles for device-grade hydrogenated amorphous silicon films and design of catalytic chemical vapor deposition apparatus," *Thin Solid Films*, vol. 395, no. 1-2, pp. 112–115, 2001.

[31] R. R. Arya, A. Catalano, and R. S. Oswald, "Amorphous silicon p-i-n solar cells with graded interface," *Applied Physics Letters*, vol. 49, no. 17, pp. 1089–1091, 1986.

[32] A. Tabata, T. Nakajima, T. Mizutani, and Y. Suzuoki, "Preparation of wide-gap hydrogenated amorphous silicon carbide thin films by hot-wire chemical vapor deposition at a low tungsten temperature," *Japanese Journal of Applied Physics, Part 2: Letters*, vol. 42, no. 1, pp. L10–L12, 2003.

[33] S. Miyajima, A. Yamada, and M. Konagai, "Characterization of undoped, N- and P-type hydrogenated nanocrystalline silicon carbide films deposited by hot-wire chemical vapor deposition at low temperatures," *Japanese Journal of Applied Physics, Part 1: Regular Papers and Short Notes and Review Papers*, vol. 46, no. 4, pp. 1415–1426, 2007.

[34] J. I. Owen, J. Hüpkes, H. Zhu, E. Bunte, and S. E. Pust, "Novel etch process to tune crater size on magnetron sputtered ZnO:Al," *Physica Status Solidi (A) Applications and Materials Science*, vol. 208, no. 1, pp. 109–113, 2011.

[35] H. Sai, H. Fujiwara, M. Kondo, and Y. Kanamori, "Enhancement of light trapping in thin-film hydrogenated microcrystalline Si solar cells using back reflectors with self-ordered dimple pattern," *Applied Physics Letters*, vol. 93, no. 14, Article ID 143501, 2008.

[36] A. V. Shah, H. Schade, M. Vanecek et al., "Thin-film silicon solar cell technology," *Progress in Photovoltaics: Research and Applications*, vol. 12, no. 2-3, pp. 113–142, 2004.

[37] M. L. Addonizio and A. Antonaia, "Surface morphology and light scattering properties of plasma etched ZnO:B films grown by LP-MOCVD for silicon thin film solar cells," *Thin Solid Films*, vol. 518, no. 4, pp. 1026–1031, 2009.